ORIGINAL

A. F. Ghaleb · **Ethar A. A. Ahmed** · **A. A. Mosharafa**

One-dimensional nonlinear model of generalized thermo-electroelasticity

Abstract We investigate a one-dimensional restriction of a nonlinear model of thermo-electroelasticity in extended thermodynamics and in the quasi-electrostatic regime (see Ghaleb et al. in Int J Eng Sci 119:29–39, 2017. https://doi.org/10.1016/j.ijengsci.2017.06.010). An additional dependence of the thermal conductivity and the thermal relaxation time on temperature and heat flux is introduced. The aim of the present work is to assess the effect of some quadratic nonlinear couplings between the mechanical, thermal and electric fields. Such couplings are known to have a crucial effect on the stability of the solutions. It is confirmed that there are two speeds of wave propagation of disturbances, the coupled thermoelastic wave and the heat wave. Formulae are provided for both speeds, showing their explicit dependence on temperature, heat flux and electric field. The purely thermal case is briefly considered. The present results may be useful for the description of a broad range of interactions in large polarizable slabs of electro-thermoelastic materials and for the design of such materials.

Abbreviations

Quantity	Description
ρ	Material density in the reference configuration
ϵ_{KL}	Dielectric tensor
β_{IJK}	Dependence of dielectric tensor on electric field
γ_{IJK}	Dependence of permanent electric displacement on strain
β_K^*	Dependence of specific entropy on electric field
ζ_K	Dependence of specific heat capacity on electric field
κ_{IJKL}	Dependence of dielectric tensor on strain
ζ_{IJKLM}	Quadratic dependence of permanent electric displacement on strain
β_{KJ}^*	Dependence of dielectric tensor on temperature
γ_{IJK}^*	Dependence of thermoelastic tensor on electric field
C_{IJKLM}	Stiffness tensor
α_{KL}	Thermoelastic tensor

A. F. Ghaleb (✉) · A. A. Mosharafa
Department of Mathematics, Faculty of Science, Cairo University, Giza 12613, Egypt
E-mail: afghaleb@sci.cu.edu.eg

E. A. A. Ahmed
School of Engineering and Applied Sciences, Nile University, Giza 12588, Egypt

γ'_{KLM}	Piezoelectric tensor
C'_{IJKLMN}	Second-order stiffness tensor
ζ'_{IJKLM}	Dependence of piezoelastic tensor on strain
κ'_{IJKL}	Electrostriction tensor
C'_{IJKL}	Dependence of stiffness tensor on temperature and thermoelastic tensor on strain
γ'^*_{ILK}	Involves γ^*_{IJK} and dependence of remanent polarization on temperature
α'^*_{KL}	Quadratic dependence of stress on temperature
C_T	Specific heat capacity
α'_{IJKL}	Quadratic dependence of entropy on strain
α^*_{KL}	Dependence of thermoelastic tensor on temperature and heat capacity on strain
A_{KL}	Quadratic dependence of free energy on heat flux
τ_h	Thermal relaxation time
t_1	Dependence of thermal relaxation time on temperature
t_2	Dependence of thermal relaxation time on heat flux
k_1	Dependence of thermal conductivity on temperature
k_2	Dependence of thermal conductivity on heat flux

1 Introduction

Thermo-electroelasticity has been a subject of both theoretical and practical importance, because it involves interactions between three fields: thermal, electric and mechanical. The various thermo-electromechanical couplings between these fields have found interesting applications in the design and performance improvement of many new structures and devices involving materials with complex composition and working in highly nonlinear regimes. Ferroelectrics and elastomers are examples of such media. These materials have attracted interest because of their various applications as actuators, in refrigeration technology and in biomedicine.

Extensive work on nonlinear electroelasticity and thermo-electroelasticity in classical thermodynamics exists in the literature. This includes review expositions, general models and applications aimed at studying the effects of nonlinear couplings (see, for example, [1–9]).

Nonlinear thermo-electroelasticity in extended thermodynamics has witnessed a growing popularity in the past few decades because of its ability to describe heat wave propagation in materials of practical interest. It allows to extend our knowledge of the different material properties, for example ferroelectricity, to new scales of length and time, and hence to produce new types of materials. Coleman et al. [10–12] investigated the implications of the second law of Thermodynamics for the constitutive relations for which the free energy depends on heat flux, in addition to temperature, as an independent thermodynamical variable. Chandrasekharaiah [13] developed a model for piezoelectric materials with the heat flux taken as an independent state variable. He et al. [14] studied the dynamic thermal and elastic responses of a piezoelectric rod subjected to a moving heat source under Lord and Shulman generalized thermo-elastic theory with one relaxation time. Babaei and Chen [15] investigated the dynamic response of a thermopiezoelectric rod to a moving heat source under Lord and Shulman theory of generalized thermoelasticity. Montanaro [16] investigated the constitutive relations for an electrically polarizable and heat conducting elastic continuum with second sound. Ghaleb [17] presented a fully nonlinear model for electrically polarizable, heat conducting elastic continuous media including several couplings between the mechanical, thermal and electric fields in the quasi-electrostatic approximation and within the frame of extended thermodynamics. Kuang [18] considered two- and three-dimensional models of electroelasticity for complex materials allowing for the existence of heat waves. Montanaro [19] used a Green–Naghdi approach to investigate the nonlinear constitutive relations of piezoelectric ceramics for which the piezoelectric moduli depend on strain. One of the presented three theories has a dependence of the free energy on heat flux. Giorgi and Montanaro [20] investigated nonlinear thermo-electroelasticity using a Green–Naghdi approach. Mehnert et al. [21] formulated a thermodynamically consistent constitutive framework of coupled thermo-electro-elasticity, with an analytic solution of a non-homogeneous boundary-value problem to illustrate the influence of various thermo-electro-mechanical couplings. A numerical modelling of thermo-electro-elasticity was presented in [22]. Kuang [23] discussed some extensions of energy principles in classical and continuum thermodynamics, e.g. the inertial heat and inertial entropy concepts and the temperature wave equation. Montanaro [24] extended the Green–Naghdi theoretical approach for thermoelasticity to thermoelectro-mechanical simple materials with fading memory that are electrically polarizable. Ghaleb et al. [25] proposed a model exhibiting thermo-electro-mechanical couplings in extended thermodynamics. This

fully nonlinear model involves a multitude of quadratic couplings, and was formulated in material coordinates, a fact that makes the resulting equations useful for the investigation of cases where the electrodes are attached to the medium. Simplified versions for thermoelasticity and for thermo-electroelasticity were investigated in [26,27]. Chirilă et al. [28] developed a thermo-electro-mechanical continuum theory for biomedical purposes following a Green–Naghdi approach to thermodynamics. The well-posedness of the mathematical model was proved. Vatulyan et al. [29] discussed an inverse problem for the determination of material coefficients in pyroelectrics. Mahmoud et al. [30] presented nonlinear, one-dimensional equations of generalized thermodynamics to treat heat wave propagation in rigid thermal conductors. Zeverdejani and Kiani [31] investigated a problem of functionally graded material in the nonlinear generalized thermoelasticity under Lord and Shulman theory. These authors commented on the importance of nonlinearity in evaluating the stresses in the material. Mirparizi et al. [32] investigated nonlinear thermoelastic, transient responses and thermal wave propagation in functionally graded solids undergoing large deformations under a thermal shock and surface stress loading in Lagrangian formulation. Jani and Kiani [33] considered the generalized thermoelastic response of a finite hollow disk made of a piezoelectric material under Lord and Shulman theory. Shakeriaski, Salehi and Ghodrat [34,35] studied the nonlinear responses in thermoelastic media under Lord and Shulman model of extended thermodynamics. These authors considered several thermal and mechanical nonlinearities, among which the dependence of the coefficient of heat conduction on temperature. Luo et al. [36] studied finite strain theory in application to the generalized coupled thermoelasticity of isotropic one-dimensional structures. These authors commented on the effects of nonlinearity of the model. Karmakar et al. [37] investigated wave scattering at the loosely bonded interface of two dissimilar rotating magneto-thermoelastic media under nonlinear thermoelasticity and dual-phase-lag model. Existence of smooth solutions and blowup of solutions of nonlinear problems of thermodynamics and thermoelasticity within extended thermodynamics were investigated in [38,39].

The available literature on the subject of generalized electro-thermoelasticity clearly indicates the growing interest in exploring the response of new generations of materials to different stimuli, for example temperature, electromagnetic fields, rotation, applied shocks, etc., in view of various applications (C.f. [31,36]). Expressed differently, the exploration of electro-thermoelastic couplings and the determination of the corresponding material coefficients have become the main target of many investigations. The present work should be situated within this context. It aims at investigating the model presented in [25] in more detail and in a one-dimensional setting, in order to assess the effect of the different nonlinear couplings on the behavior of the medium under thermal load. Nonlinearity may be geometrical when the body undergoes large deformations, or physical as the different material parameters may be dependent on strain, temperature and electric field, or else arising from the implications of extended thermodynamics (C.f. [12]). This is of primordial importance for the design of materials for special purposes in which nonlinear effects are essential in evaluating the response of the material, for example in the field of thermo-electromechanical actuators (multi-trigger actuators) in which there is coupling between the three fields [40,41].

Formulae are derived for the speeds of the coupled thermoelastic wave and the heat wave, showing explicit dependence on temperature, heat flux and electric field. These formulae may be compared with available experimental data to determine some material constants of the medium. As illustration, we solve a one-dimensional boundary-value problem for the half-space in the quasi-electrostatic approximation and under thermal load at the boundary and initially at rest. The linear purely thermal case is briefly considered, in order to point out at the difficulties facing the evaluation of solutions even in the simplest case. Then the full nonlinear problem is investigated numerically using a simple, explicit finite-difference technique devised by the authors and used efficiently in previous work.

As presented below, the model contains a large number of coupling constants, up to second degree included. Considering the effect of each one of them separately would amount to a most difficult task and make the work exceedingly long. In fact, we have disregarded some of them from the outset, as these have been investigated somewhere else, and concentrated on the rest of them.

Three cases are considered, for which different values of the material constants are chosen. Some other constants will retain their values throughout the cases. During the calculations, some of the considered coupling constants will assume small enough values, by which their effect will be negligible in the numerical outcome.

Two- and three-dimensional plots corresponding to these three cases are provided and discussed. In doing so, our choices of the different parameters aimed at obtaining comparable speeds for the coupled thermoelastic wave and for the heat wave in order to put in evidence the interaction of both waves. In solving the problem numerically, as is usually done for finite-difference schemes, an artificial far boundary had to be considered, at which all unknown functions identically vanish, so as not to take in consideration any reflected waves.

2 Basic three-dimensional equations

The basic features of the model under consideration is the introduction of the heat flux as an additional thermodynamical variable, together with the strain and the electric field. A Cattaneo-type evolution equation for the heat flux is assumed, in replacement of the classical Fourier law for heat conduction. Additionally, a linear dependence of the heat wave speed on temperature and heat flux is introduced. The proposed form of the free energy involves many of the usual thermo-electro-mechanical couplings, keeping only nonlinear terms up to the second degree included, in addition to a quadratic dependence on the heat flux as suggested in [11]. The nonlinearities involved in the system of basic equations arise from different sources: They may be of geometrical origin as the body can undergo large deformations, or physical through the dependence of the different material parameters on the unknown functions like temperature, strain, heat flux and electric field, or else from the implications of extended thermodynamics as the free energy of the body has a quadratic dependence on heat flux as stated earlier. The model accounts, among others, for residual polarization (ferroelectricity) which depends on various parameters, and for pyroelectric and electrocaloric effects which usually have a strong dependence on temperature (C.f. [42]). The electrocaloric effect can have important applications in new materials (C.f. [43,44]). All of the other couplings may be considered in detail. For example, the dependence of entropy on electric field is found to be experimentally detectable only for sufficiently large electric fields of the order of $10^3 \, V/m$, a value that is in the range of nonlinear dielectric response (C.f. [45]). Importance of accounting for the dependence of material coefficients on temperature in piezoelectric composite materials is reported in [46]. Abundant literature exists on the design of new materials and their material properties (see, for example, [47,48]). Mechanical and electric hystereses are disregarded. As to the dissipation function, it is a positive semi-definite quadratic form in the components of the heat flux. Thus the present model does not include the Green–Naghdi theories of types II and III which are characterized by the absence of dissipation. It does not include the Green–Lindsay theory of generalized thermoelasticity as well, in view of the hypotheses in the model. This becomes clear in the purely thermal case, noting that the heat equation (34) does not involve a third order derivative of temperature. It goes without saying that the model is thermodynamically consistent. Details may be found in [25]. Parent one-dimensional nonlinear models of thermodynamics and thermoelasticity with second sound in which the material coefficients may depend on strain and temperature were treated for the existence of smooth solutions and blowup of solutions in [38,39].

After incorporating the constitutive relations into the field equations and disregarding the external forces and the heat supply, one is left with the final set of three-dimensional field equations involving eight basic unknown functions: three mechanical displacement components U_K, the temperature θ as measured from a reference temperature, three components of the heat flux Q_K and the electric potential Φ.

In the following equations, a "comma" is used to denote differentiation w.r.to the material coordinates. Written down in material coordinates following [25], the basic system of governing partial differential equations to be investigated below reads:

(i) **The equation of electrostatics:**

$$
\begin{aligned}
&-\epsilon_{KJ}\Phi_{,JK} + 3\rho\beta_{IJK}\left(\Phi_{,IK}\Phi_{,J} + \Phi_{,I}\Phi_{,JK}\right) \\
&+\rho\gamma_{IJK}U_{I,JK} + \rho\beta_K^*\theta_{,K} - 2\rho\zeta_K\theta\theta_{,K} \\
&+\varepsilon_0\left(U_{L,KK}\Phi_{,L} + U_{L,K}\Phi_{,LK}\right) - \varepsilon_0\left(U_{S,SK}\Phi_K + U_{S,S}\Phi_{,KK}\right) \\
&+\varepsilon_0\left(U_{K,LK}\Phi_{,L} + U_{K,L}\Phi_{,LK}\right) + 2\rho\kappa_{IJKL}\left(\Phi_{,LK}U_{I,J} + \Phi_{,L}U_{I,JK}\right) \\
&-\frac{1}{2}\rho\gamma_{IJK}(U_{M,IK}U_{M,J} + U_{M,I}U_{M,JK}) - \frac{1}{2}\rho\zeta_{IJKLM}(U_{I,JK}U_{M,L} + U_{I,J}U_{M,LK}) \\
&-\frac{1}{2}\rho\zeta_{IJKLM}(U_{I,JK}U_{L,M} + U_{I,J}U_{L,MK}) \\
&-\rho\theta_{,K}\left(-2\beta_{KJ}^*\Phi_{,J} + \gamma_{IJK}^*U_{I,J}\right) - \rho\theta\left(-2\beta_{KJ}^*\Phi_{,JK} + \gamma_{IJK}^*U_{I,JK}\right) = 0
\end{aligned}
\tag{1}
$$

(ii) **The equations of motion:**

$$
\begin{aligned}
\rho\frac{\partial^2 U_L}{\partial t^2} = &\, C_{IJKL}U_{I,JK} - \alpha_{KL}\theta_{,K} - \gamma_{KLM}'\Phi_{,MK} \\
&+C_{IJKLMN}'U_{I,JK}U_{M,N} + C_{IJKLMN}'U_{I,J}U_{M,NK} \\
&-\zeta_{IJKLM}'U_{I,JK}\Phi_{,M} - \zeta_{IJKLM}'U_{I,J}\Phi_{,MK}
\end{aligned}
$$

$$+\kappa'_{IJKL}\Phi_{,IK}\Phi_{,J} + \kappa'_{IJKL}\Phi_{,I}\Phi_{,JK}$$
$$+C'_{IJKL}U_{I,JK}\theta + C'_{IJKL}U_{I,J}\theta_{,K}$$
$$-\gamma'^*_{ILK}\theta\Phi_{,IK} - \gamma'^*_{ILK}\Phi_{,I}\theta_{,K} + 2\alpha^*_{KL}\theta\theta_{,K}. \tag{2}$$

(iii) **The equation of energy:**

$$\rho\Theta\left[\alpha_{IJ}\dot{U}_{I,J} - \beta^*_I\dot{\Phi}_{,I} + \frac{C_T}{\theta_0}\dot{\theta}\right.$$
$$- \left(\alpha'_{IJKL} + \alpha'_{KLIJ}\right)\dot{U}_{I,J}U_{K,L} - \left(\beta^*_{IJ} + \beta^*_{JI}\right)\dot{\Phi}_{,I}\Phi_{,J}$$
$$-2\alpha^*_{IJ}\left(\dot{\theta}U_{I,J} + \theta\dot{U}_{I,J}\right)$$
$$\left.+ 2\zeta_J\left(\dot{\theta}\Phi_{,J} + \theta\dot{\Phi}_{,J}\right) + \gamma^*_{IJK}\left(\dot{U}_{I,J}\Phi_{,K} + U_{I,J}\dot{\Phi}_{,K}\right)\right]$$
$$= -\Theta\left(\frac{Q_K}{\Theta}\right)_{,K} + A_{MR}Q_MQ_R \tag{3}$$

(iv) **The Cattaneo evolution equation for the heat flux:**

$$\rho\Theta\,\tau_h\,\dot{Q}_L = -Q_L - A^{-1}_{LS}\theta_{,S}, \tag{4}$$

and tensor A is identified with the inverse of the heat conduction tensor K:

$$A = K^{-1}$$

.

The electric induction vector

$$\bar{D}_K = \varepsilon_0 J X_{K,i} X_{L,i}\bar{E}_L + \bar{P}_K \tag{5}$$

is finally obtained as:

$$\bar{D}_K = \bar{D}^0_K + \varepsilon_{KL}\bar{E}_L, \tag{6}$$

with

$$\bar{D}^0_K = -\rho\beta_K + \rho_R\beta^*_K\theta + \rho\gamma_{IJK}U_{I,J} - \rho\zeta_K\theta^2$$
$$+\frac{1}{2}\rho\gamma_{IJK}U_{M,I}U_{M,J} - \frac{1}{2}\rho\zeta_{IJKLM}U_{I,J}U_{M,L} - \frac{1}{2}\rho\zeta_{IJKLM}U_{I,J}U_{L,M}$$
$$-\rho\gamma^*_{IJK}\theta U_{I,J} \tag{7}$$
$$\varepsilon_{KL} = \epsilon_{KL} - 2\rho\beta^*_{KL}\theta - 3\rho\beta_{IKL}\bar{E}_I$$
$$-2\varepsilon_0 U_{L,K} + \varepsilon_0 U_{S,S}\delta_{KL} - 2\rho\kappa_{IJKL}U_{I,J}, \tag{8}$$

where

$$\epsilon_{KL} = \varepsilon_0\delta_{KL} - 2\rho\beta_{KL} \tag{9}$$

The material electric field and electric induction are endowed with a "bar", the meanings of the coupling constants are explained in Nomenclature. Details of the derivation may be found in [25]. For the definition of material electromagnetic quantities, the reader is referred to [1].

The system of equations (1)–(4) is not pure "hyperbolic" due to the equation of electrostatics expressed in the quasi-electrostatic approximation. However, if one adds to this equation a term involving the time derivative of the electric potential endowed with a small multiplicative positive parameter and takes the limit of the solution as this parameter tends to zero, then one may assume that the considered system of equations is of mixed "hyperbolic-parabolic" type. This means that the solution will partly have a diffusive character, side by side with its wave nature.

Relying on the above equations, it is thus clear that the model accounts for both ferroelectricity and pyroelectricity, and for the dependence of the different material parameters on strain, temperature and electric field. In particular, the spontaneous polarization has a dependence on strain and temperature.

One-dimensional models have been extensively and efficiently used to describe a multitude of physical phenomena in large slab or half-space. We only cite a few for the sake of conciseness: Sherief and Dhaliwal [49] studied the one-dimensional problem of a thermoelastic half-space subjected to sudden heating in extended thermodynamics. Gryza and Kosłowski [50,51] proposed analytical and numerical solutions to one-dimensional boundary-value problems in thermoelastic slabs. New aspects of the solutions could be obtained using such simplified models. Chandrasekharaiah [52] obtained exact solutions in closed form to the one-dimensional problem of wave propagation in a half-space in the linear theory of thermoelasticity without energy dissipation.

Nonlinear, one-dimensional models of pure thermodynamics or thermoelasticity with second sound and various dependences of the material coefficients on strain, temperature and heat flux may be found in [36,38,39].

In what follows, we shall consider a one-dimensional version of the basic equations for simplicity, then introduce a dimension analysis that will reduce the speed of the heat wave in the linear case to unity. Understandably, the speed of the coupled thermoelastic wave in this case is expected to be less than unity, but the choices of the characteristic parameters will be made in a way so as to make the two speeds comparable to each other in magnitude. We believe that such choice may be useful in studying the interactions between the heat wave and the coupled thermoelastic wave.

By writing the basic equations in alternative forms, it is possible to extract expressions showing the dependence of the two speeds of wave propagation on strain, temperature, heat flux and electric field. Comparing these expressions with available experimental data allows to determine some material parameters.

As already noted, the model contains a multitude of coupling constants, whether linear or quadratic nonlinear. Instead of looking separately for the effect of each material parameter on the response of the material, three choices of the set of material parameters are considered, in which the values of one and the same coefficient may differ by several orders of magnitude from one case to the other. Some of these parameters will retain their values throughout the three cases. In doing so, we will not have in mind a concrete medium. This way of dealing with the nonlinear couplings will allow to assess globally the effect of the material parameters on the electro-thermomechanical response of the medium. Each case will correspond to definite values of the two speeds of wave propagation.

Then we shall consider the purely thermal problem analytically by small parameter expansion in order to put in evidence the difficulties to be met for obtaining such solutions, before tackling the full nonlinear system of equations numerically. For the latter approach, it is worth mentioning that the solutions could be obtained only for relatively small time values due to lack of stability of the used explicit, finite-difference numerical scheme.

3 One-dimensional equations

In order to concentrate on the main goal of the present work, the equations are now written in one spatial dimension. Moreover, all the terms with the interactions $U - U$ and $U - \Phi$ have been deleted for conciseness. The unknown functions are now U, θ, Q, Φ. These unknowns satisfy a set of four coupled partial differential equations: The equation of Electrostatics, the equation of motion, the equation of energy and Cattaneo-like evolution equation for the heat flux.

$$
\begin{aligned}
&-\epsilon \frac{\partial^2 \Phi}{\partial x^2} + 6\rho\beta \left(\frac{\partial \Phi}{\partial x} \frac{\partial^2 \Phi}{\partial x^2} \right) + \rho\gamma \frac{\partial^2 U}{\partial x^2} + \rho\beta^\star \frac{\partial \theta}{\partial x} - 2\rho\zeta\theta \frac{\partial \theta}{\partial x} \\
&- \rho \frac{\partial \theta}{\partial x} \left(-2\beta^\star \frac{\partial \Phi}{\partial x} + \gamma^\star \frac{\partial U}{\partial x} \right) - \rho\theta \left(-2\beta^\star \frac{\partial^2 \Phi}{\partial x^2} + \gamma^\star \frac{\partial^2 U}{\partial x^2} \right) = 0,
\end{aligned}
\tag{10}
$$

$$
\begin{aligned}
\rho \frac{\partial^2 U}{\partial t^2} &= C_E \frac{\partial^2 U}{\partial x^2} - \alpha \frac{\partial \theta}{\partial x} - \gamma' \frac{\partial^2 \Phi}{\partial x^2} + C' \left(\theta \frac{\partial^2 U}{\partial x^2} + \frac{\partial U}{\partial x} \frac{\partial \theta}{\partial x} \right) \\
&+ 2\kappa' \frac{\partial \Phi}{\partial x} \frac{\partial^2 \Phi}{\partial x^2} - \gamma'^\star \theta \frac{\partial^2 \Phi}{\partial x^2} - \gamma'^\star \frac{\partial \theta}{\partial x} \frac{\partial \Phi}{\partial x} + 2\alpha^\star \theta \frac{\partial \theta}{\partial x},
\end{aligned}
\tag{11}
$$

$$
\begin{aligned}
\rho\theta_0 &\left[\alpha \frac{\partial^2 U}{\partial x \partial t} - \beta^\star \frac{\partial^2 \Phi}{\partial x \partial t} - 2B^\star \frac{\partial^2 \Phi}{\partial x \partial t} \frac{\partial \Phi}{\partial x} + \frac{C_T}{\theta_0} \frac{\partial \theta}{\partial t} + 2\zeta \left(\frac{\partial \theta}{\partial t} \frac{\partial \Phi}{\partial x} + \theta \frac{\partial^2 \Phi}{\partial x \partial t} \right) \right] \\
&+ \rho\theta \left(\alpha \frac{\partial^2 U}{\partial x \partial t} - \beta^\star \frac{\partial^2 \Phi}{\partial x \partial t} + \frac{C_T}{\theta_0} \frac{\partial \theta}{\partial t} \right) - 2\alpha^\star \left(\frac{\partial \theta}{\partial t} \frac{\partial U}{\partial x} + \theta \frac{\partial^2 U}{\partial x \partial t} \right)
\end{aligned}
$$

$$= -\frac{\partial Q}{\partial x} + \frac{1}{\theta_0} Q \frac{\partial \theta}{\partial x} + \frac{1}{K_0 \theta_0} Q^2, \tag{12}$$

$$\rho \tau_h (\theta_0 + \theta) \frac{\partial Q}{\partial t} = -Q - K \frac{\partial \theta}{\partial x}. \tag{13}$$

The electric induction component is finally obtained as:

$$\bar{D} = \bar{D}^0 - \varepsilon \frac{\partial \Phi}{\partial x}, \tag{14}$$

with

$$\bar{D}^0 = -\rho \beta + \rho \beta^* \theta + \rho \gamma \frac{\partial U}{\partial x} - \rho \zeta \theta^2 - \rho \gamma^* \theta \frac{\partial U}{\partial x} \tag{15}$$

$$\varepsilon = \varepsilon_0 - 2\rho\beta - 2\rho\beta^*\theta + 3\rho\beta \frac{\partial \Phi}{\partial x} - (\varepsilon_0 + 2\rho\kappa) \frac{\partial U}{\partial x}, \tag{16}$$

Strain-, temperature- and electric field-dependences of the dielectric constant and other material coefficients were frequently reported in the literature (C.f. [53,54]).

As a generalization of the model proposed in [25], we introduce a linear dependence of the heat conduction coefficient and the thermal relaxation time on temperature and heat flux. This does not alter in any way the thermodynamical consistency of the model:

$$K = K_0 (1 + k_1 \theta + k_2 Q) \tag{17}$$

and

$$\tau_h = \tau_0 (1 + t_1 \theta + t_2 Q). \tag{18}$$

Various dependences of the thermal relaxation time and the other material coefficients on strain, temperature and heat flux have been presented in [38,39].

4 Dimension analysis

No definite material was chosen for the purpose of numerical evaluations. Instead, our main goal was to include as many nonlinear couplings parameters as possible, and to put in evidence the propagation two waves, the coupled thermoelastic wave (slow) and the heat wave (fast), so that the difference in speeds is not too large. Three cases are considered for the numerical application. The values of the various material constants are shown in Table 1:

The characteristic parameters of length, time, heat flux and electric potential are as follows:

$$L_0 = \frac{\theta_0 K_0}{Q_0}, \quad T_0 = \rho \theta_0 \tau_0, \quad Q_0 = \sqrt{\frac{\theta_0 C_T K_0}{\tau_0}}, \quad \Phi_0 = \frac{\rho L_0^3}{\gamma' T_0^2}. \tag{19}$$

For the used set of material coefficients one has:

Cases II and III have much larger values of the specific heat capacity and the coefficient of linear thermal expansion, and much smaller values of the characteristic time and length, as compared to Case I. Again, Case II has much larger values of the coefficients γ', $\gamma'^\star$ ζ and κ', and much smaller values for the coefficients $\beta^\star$, γ and $\gamma^\star$, as compared to the other two cases.

Carrying out the dimension analysis, the basic equations are cast in a more convenient form to show the dependence of the various coupling constants on temperature, heat flux and electric field:

$$-\left(1 - 2\frac{\rho\theta_0\beta^\star}{\epsilon}\theta - \frac{6\rho\beta\Phi_0}{\epsilon L_0} \frac{\partial\Phi}{\partial x}\right)\frac{\partial^2\Phi}{\partial x^2} + \left(\frac{\rho\gamma L_0}{\epsilon\Phi_0} - \frac{\rho\theta_0\gamma^\star L_0}{\epsilon\Phi_0}\theta\right)\frac{\partial^2 U}{\partial x^2}$$

$$+\left(\frac{\rho\theta_0\beta^\star L_0}{\epsilon\Phi_0} - 2\frac{\rho\zeta\theta_0^2 L_0}{\epsilon\Phi_0}\theta - \frac{\rho\theta_0\gamma^\star L_0}{\epsilon\Phi_0}\frac{\partial U}{\partial x} + 2\frac{\rho\theta_0\beta^\star}{\epsilon}\frac{\partial\Phi}{\partial x}\right)\frac{\partial\theta}{\partial x} = 0, \tag{20}$$

Table 1 Values of the material parameters

Quantity	Unit	Case I	Case II	Case III
C_E	N m^{-2}	3.46×10^{10}	0.246×10^{10}	5.46×10^{10}
C_T	J kg^{-1} K^{-1}	0.3×10^5	0.4×10^8	1.6×10^7
C'	kg m^{-1} s^{-2} K^{-1}	0.3×10^5	0.4×10^5	1.6×10^5
K_0	W m^{-1} K^{-1}	1.0×10^4	1.0×10^4	1.0×10^4
α	J kg^{-1} K^{-1}	0.5×10^5	0.4×10^8	1.5×10^7
$\alpha^\star$	kg m^{-1} s^{-2} K^{-2}	0.2×10^6	0.1×10^6	0.5×10^6
β	Coul m^4 kg^{-1} J^{-1}	0.1×10^{-13}	0.1×10^{-13}	0.1×10^{-13}
$\beta^\star$	m^3 kg^{-1} K^{-1}	0.9×10^{-6}	0.1×10^{-9}	0.1×10^{-6}
γ	m^3 kg^{-1}	0.5×10^5	0.3×10^3	0.3×10^5
γ'	Coul m^{-2}	0.1×10^3	0.2×10^5	0.2×10^3
$\gamma^\star$	m^2 J kg^{-1} K^{-1} Coul^{-1}	0.5×10^3	1.0	0.1×10^3
$\gamma'^\star$	Coul m^{-2} K^{-1}	0.1	0.2×10^2	0.2
ϵ		2.0	2.0	2.0
ζ	m^3 kg^{-1} K^{-2}	0.1×10^{-7}	0.3×10^{-2}	1.3×10^{-5}
θ_0	K	293	293	293
κ'	Coul^2 kg^{-1} m^{-3} s^2	0.2×10^{-7}	0.5×10^{-3}	1.0×10^{-7}
ρ	kg m^{-3}	8954	8954	8954
τ_0	s m^3 kg^{-1} K^{-1}	0.5×10^{-18}	0.1×10^{-20}	0.8×10^{-21}

Table 2 Values of the characteristic parameters

Quantity	Unit	Case I	Case II	Case III
L_0	m	0.69×10^{-10}	8.559×10^{-12}	1.210×10^{-11}
T_0	s	1.31×10^{-12}	2.623×10^{-15}	2.099×10^{-15}
Q_0	W m^{-2}	0.42×10^{15}	3.422×10^{17}	2.421×10^{17}
Φ_0	volt	0.18×10^2	0.407783×10^{-4}	1.802×10^{-2}

$$\frac{\partial^2 U}{\partial t^2} = \left(v_e^2 + C'\gamma_0\theta_0\,\theta\right)\frac{\partial^2 U}{\partial x^2} - \left(\alpha\theta_0\gamma_0 - 2\alpha^\star\gamma_0\theta_0^2\,\theta + C'\gamma_0\theta_0\frac{\partial U}{\partial x} + \frac{\gamma'^\star\theta_0}{\gamma'}\frac{\partial \Phi}{\partial x}\right)\frac{\partial \theta}{\partial x}$$

$$- \left(1 + \frac{\gamma'^\star\theta_0}{\gamma'}\theta - \frac{2\kappa'}{\gamma_0\gamma'^2}\frac{\partial \Phi}{\partial x}\right)\frac{\partial^2 \Phi}{\partial x^2}, \tag{21}$$

$$\frac{\alpha}{C_T}\left[1 + \left(1 - \frac{2\alpha^\star}{\rho\alpha}\right)\theta\right]\frac{\partial^2 U}{\partial x \partial t} + \left(1 + \theta - \frac{2\alpha^\star}{\rho C_T}\frac{\partial U}{\partial x} + 2\frac{\zeta\theta_0\Phi_0}{C_T L_0}\frac{\partial \Phi}{\partial x}\right)\frac{\partial \theta}{\partial t}$$

$$- \left[\frac{\beta^\star\Phi_0}{C_T L_0} + \left(\frac{\beta^\star\Phi_0}{C_T L_0} - 2\frac{\zeta\theta_0\Phi_0}{C_T L_0}\right)\theta + 2\frac{B^\star\Phi_0^2}{C_T L_0^2}\frac{\partial \Phi}{\partial x}\right]\frac{\partial^2 \Phi}{\partial x \partial t} = -\frac{\partial Q}{\partial x} + Q\frac{\partial \theta}{\partial x} + Q^2, \tag{22}$$

$$[1 + (1 + \tau_1)\theta + \tau_2 Q]\frac{\partial Q}{\partial t} = -Q - (1 + q_1\theta + q_2 Q)\frac{\partial \theta}{\partial x}. \tag{23}$$

Here

$$\gamma_0 = \frac{\rho\theta_0 C_T \tau_0}{K_0}, \quad [\gamma_0] = \text{kg}^{-1}\,\text{m s}^2, \quad v_e = \sqrt{C_E\gamma_0}$$

and

$$\tau_1 = t_1\theta_0, \quad \tau_2 = t_2 Q_0, \quad q_1 = k_1\theta_0, \quad q_2 = k_2 Q_0.$$

is the speed of propagation of the coupled thermoelastic wave in the linearized theory. From Eqs. (21) and (22) it is seen that the adimensionalized thermoelastic coefficient

$$\gamma_{TE} = \alpha\theta_0\gamma_0 - 2\alpha^\star\gamma_0\theta_0^2\,\theta + C'\gamma_0\theta_0\frac{\partial U}{\partial x} + \frac{\gamma'^\star\theta_0}{\gamma'}\frac{\partial \Phi}{\partial x} \tag{24}$$

Table 3 Dimensionless speed of the coupled thermoelastic wave and coefficient of linear thermal expansion

Quantity	Unit	Case I	Case II	Case III
v_e		0.37	0.16	0.43
$\alpha\theta_0\gamma_0$		0.58×10^{-4}	0.12	0.01

and specific heat capacity

$$C_T' = \left(1 - \frac{\frac{2\alpha^\star}{\rho C_T}\frac{\partial U}{\partial x} - 2\frac{\zeta\theta_0\Phi_0}{C_T L_0}\frac{\partial \Phi}{\partial x}}{1 + \theta}\right)C_T \tag{25}$$

have a dependence on temperature, strain and electric field, due to coupling effects.

The dimensionless speed of the coupled thermoelastic wave in the linearized theory and the coefficient of linear thermal expansion for the three cases under consideration are shown on Table 3:

With the used characteristic quantities, the speed of propagation of the heat wave is close to unity as verified from (22) and (23), provided its dependence on temperature and heat flux is small enough.

After some manipulations on eqs.(20) and (21) to eliminate the second spatial derivative of the electric potential, the equation of motion may be cast into the form of a wave equation with various damping terms:

$$\frac{\partial^2 U}{\partial t^2} = v_E^2 \frac{\partial^2 U}{\partial x^2} + \text{terms depending only on functions } \theta \text{ and } \Phi, \tag{26}$$

yielding the following relation for the squared velocity of propagation of the coupled thermo-electroelastic wave as function of temperature and electric field:

$$v_E^2 = \left(v_e^2 + C'\gamma_0\theta_0\,\theta\right) - \left(1 + \frac{\gamma'^\star\theta_0}{\gamma'}\,\theta - \frac{2\kappa'}{\gamma_0\gamma'^2}\,\frac{\partial \Phi}{\partial x}\right)\frac{\rho\gamma L_0}{\epsilon\Phi_0}\,\frac{1 - \frac{\theta_0\gamma^\star}{\gamma}\,\theta}{1 - \frac{3\rho\beta\Phi_0}{\epsilon L_0}\,\frac{\partial \Phi}{\partial x} + \frac{2\rho\theta_0\beta^\star}{\epsilon}\theta}. \tag{27}$$

For the present model, the velocity v_E does not depend of heat flux.

Again, by cross-differentiation in (22) and (23) and elimination of a second mixed derivative of the heat flux, one obtains:

$$\frac{\partial^2 \theta}{\partial t^2} = v_H^2 \frac{\partial^2 \theta}{\partial x^2} + \text{terms depending only on functions } U, Q \text{ and } \Phi, \tag{28}$$

which gives the squared velocity of propagation of the heat wave:

$$v_H^2 = \frac{1}{1 + \theta - \frac{2\alpha^\star}{\rho C_T}\frac{\partial U}{\partial x} + 2\frac{\zeta\theta_0\Phi_0}{C_T L_0}\frac{\partial \Phi}{\partial x}}\,\frac{1 + k_1\theta + k_2 Q}{1 + (1 + t_1)\,\theta + t_2 Q} \tag{29}$$

depending on temperature, strain, heat flux and electric field. In the linearized theory, the value of this speed is unity. Dependence of the second sound speed on heat flux was reported by Coleman and Newman [12]. A similar wave equation for Q may be obtained as well.

The above formulae for v_E and v_H have not been reported previously, and can be used in conjunction of experimental results to provide values for some material constants. They are suitable for evaluating the effect of nonlinearity on the wave speeds.

Systems of nonlinear hyperbolic equations have been investigated by many authors, among whom we cite [55–58]. In the following two sections we find solutions to our equations under some initial and boundary conditions using either Poincaré expansion or by numerical techniques.

5 The purely thermal case

A few investigations were carried out on rigid thermal conductors within the theory of extended thermodynamics, among which we cite [59,60]. In what follows, we show that the reduced equations for purely thermal problem still lead to cumbersome solutions if one tries the analytical techniques. Here the basic nonlinear one-dimensional adimensionalized equations reduce to two only for the functions of temperature $\theta(t, x)$ and heat flux $Q(t, x)$:

$$\frac{\partial \theta}{\partial t} + \theta \frac{\partial \theta}{\partial t} = -\frac{\partial Q}{\partial x} + Q \frac{\partial \theta}{\partial x} + Q^2, \tag{30}$$

$$[1 + (1 + \tau_1)\theta + \tau_2 Q] \frac{\partial Q}{\partial t} = -Q - (1 + q_1\theta + q_2 Q) \frac{\partial \theta}{\partial x}. \tag{31}$$

Let us try an expansion of the solution in terms of a small Poincaré parameter v:

$$\theta = v\theta_1 + v^2\theta_2 + \cdots, \qquad Q = vQ_1 + v^2Q_2 + \cdots. \tag{32}$$

The equations to the first-order of approximation are:

$$\frac{\partial \theta_1}{\partial t} = -\frac{\partial Q_1}{\partial x}, \qquad \frac{\partial Q_1}{\partial t} = -Q_1 - \frac{\partial \theta_1}{\partial x}, \tag{33}$$

with

$$\lim_{x \to \infty} \theta_1(t, x) = 0, \qquad \lim_{x \to \infty} \frac{\partial \theta_1(t, x)}{\partial x} = 0$$

and similar radiational conditions on the function $Q(t, x)$.

By differentiation one can easily decouple equations (33) and obtain two identical wave equations with damping for θ and Q of the form:

$$\frac{\partial^2 \theta_1}{\partial x^2} - \frac{\partial^2 \theta_1}{\partial t^2} - \frac{\partial \theta_1}{\partial t} = 0, \tag{34}$$

showing that the non-dimensional speed of the heat wave is equal to unity as expected.

We shall find a solution in the half-space with given initial and boundary conditions:

$$\theta_1(t, 0) = f_0(t), \quad Q_1(t, 0) = g_0(t), \quad \theta_1(0, x) = f_1(x), \quad Q_1(0, x) = g_1(x). \tag{35}$$

The missing initial conditions on the time rates of change may be obtained using (33):

$$\frac{\partial \theta_1}{\partial t}(0, x) = -g_1'(x), \quad \frac{\partial Q_1}{\partial t}(0, x) = -g_1(x) - f_1'(x). \tag{36}$$

Applying the Fourier sine transform with respect to the x variable:

$$\tilde{\theta}_1(t, \xi) = \int_0^\infty \theta_1(t, x) \sin(x\xi) \, dx, \tag{37}$$

to Eq. (34), one is finally led to the following solution for the transform:

$$\tilde{\theta}_1(t, \xi) = \frac{\xi}{\lambda_1 - \lambda_2} \int_0^t \left[e^{\lambda_1(t-\tau)} - e^{\lambda_2(t-\tau)} \right] f_0(\tau) \, d\tau$$
$$+ \frac{\lambda_2 \tilde{f}_1(\xi) - \tilde{G}_1(\xi)}{\lambda_2 - \lambda_1} e^{\lambda_1 t} - \frac{\lambda_1 \tilde{f}_1(\xi) + \tilde{G}_1(\xi)}{\lambda_2 - \lambda_1} e^{\lambda_2 t}. \tag{38}$$

the values λ_1 and λ_2 being the roots of the quadratic algebraic equation:

$$\lambda^2 + \lambda + \xi^2 = 0 \quad \rightarrow \quad \lambda_{1,2} = -\frac{1}{2} \pm \frac{1}{2}\sqrt{1 - 4\xi^2}, \tag{39}$$
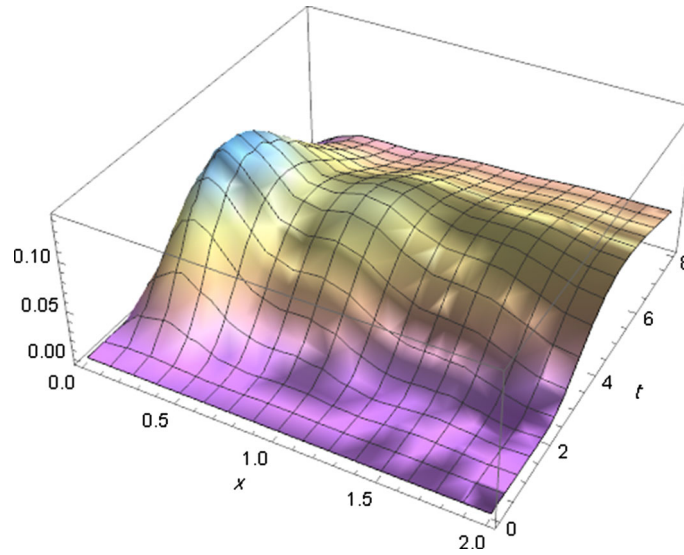
Fig. 1 $3D$-temperature distribution for the linear case

and $\tilde{f}_1(\xi)$, $\tilde{G}_1(\xi)$ are the Fourier sine transforms of $f_1(x)$ and $g_1'(x)$ respectively, whence the solution:

$$\theta_1(t, x) = \frac{2}{\pi} \int_0^\infty \tilde{\theta}_1(t, \xi) \sin(x\xi) \, d\xi, \tag{40}$$

The steps of the solution are straightforward and details have been omitted for conciseness. The solution for $Q_1(t, x)$ can be found in an analogous manner.

Turn now to the second-order solution. The system of equations reads:

$$\frac{\partial \theta_2}{\partial t} + \frac{\partial Q_2}{\partial x} = F(t, x), \qquad \frac{\partial Q_2}{\partial t} + Q_2 + \frac{\partial \theta_2}{\partial x} = G(t, x), \tag{41}$$

with

$$F(t, x) = -\theta_1 \frac{\partial \theta_1}{\partial t} + Q_1 \frac{\partial \theta_1}{\partial t} + Q_1^2, \tag{42}$$

$$G(t, x) = -(1 + \tau_1)\theta_1 \frac{\partial Q_1}{\partial t} + \tau_2 Q_1 \frac{\partial Q_1}{\partial t} - q_1 \theta_1 \frac{\partial \theta_1}{\partial x} + q_2 Q_1 \frac{\partial \theta_1}{\partial x} \tag{43}$$

Equations (41) can be solved using exactly the same technique as for the first-order approximation, the only difference being the existence of the non-homogeneous terms on the r.h.s. of the equations. The solution is quite cumbersome and is expressed in terms of a quadruple integral. We shall refrain from writing down the second-order solution. The complexity of the calculations makes a case in favour of the numerical methods of solution.

When the initial conditions are set to zero, the obtained solution to the first order represents the propagation of the boundary regime. This is illustrated in Figs. 1 and 2 for the boundary regime:

$$f_0(t) = 0.1 \, t^3 \, e^{-t}, \tag{44}$$

where we have shown the three-dimensional distribution of temperature in the half-space, and the temperature as function of time at the location $x = 1$. Notice the time lag needed for the heat wave to reach location $x = 1$, and that the wave amplitude at this location ($\simeq 0.1$) is smaller than the amplitude of the boundary regime ($\simeq 0.134$). Temperature is non-negative everywhere in compliance with the laws of thermodynamics as expected. As the heat flux is much smaller than temperature in absolute value, we have verified that the nonlinear solution for this boundary regime is almost identical to the linear one for the considered time values $t \leq 1$. Deviations between the two solutions may become more substantial as time grows.
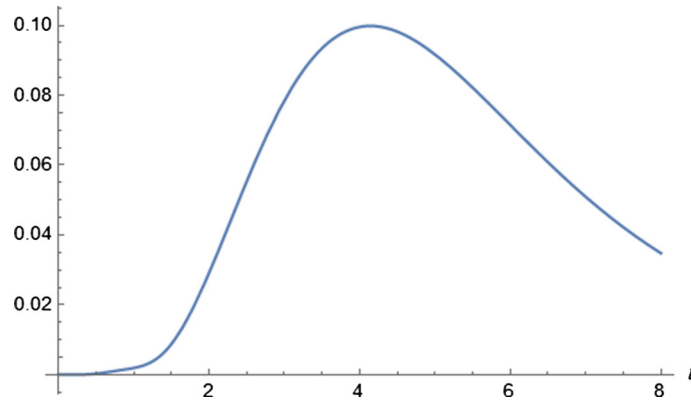
Fig. 2 Temperature distribution for the linear case at location $x = 1$
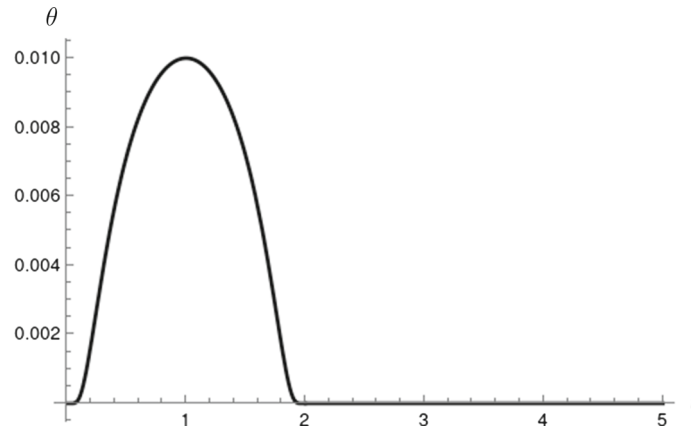
Fig. 3 Temperature distribution at the boundary as function of time for the nonlinear problem

6 Numerical results for the nonlinear problem by finite differences

For all the following numerical calculations for the nonlinear problem, the initial conditions are set to zero. We consider the propagation of a continuous heating boundary regime in a half-space $x \geq 0$, with prescribed finite-support temperature at the boundary of the form:

$$\theta(0, t) = \begin{cases} 0.1\, e^{-\frac{(t-1)^2}{1-(t-1)^2}}, & 0 \leq t \leq 2 \\ 0, & t > 2, \end{cases} \tag{45}$$

The plot of this smooth function is shown in Fig. 3.

Initially at time $t = 0$ the medium was in complete rest at temperature θ_0 and at zero electric potential. At the boundary $x = 0$, all boundary conditions for displacement, heat flux and electric potential are set equal to zero. At the computational far end, all four unknown solution functions are set equal to zero.

A simple explicit, three-level finite difference scheme is used to solve the set of nonlinear equations (20)–(23). Taking the steps along axes to be Δx, Δt, the grid points are labeled as:

$$x_i = (i-1)\Delta x, \quad t_k = (k-1)\Delta t, \quad i, k = 1, 2, \ldots$$

For computations, we have taken

$$\Delta x = 0.1, \quad \Delta t = 0.05.$$

Let $F(x_i, t_k) \simeq F_{i,k}$, where $F_{i,k}$ is an approximate value of function F at the node (x_i, t_k), (i, k) for short. The different derivatives needed in the sequel are discretized by central differences as:

$$\frac{\partial F}{\partial x} = \frac{F_{i+1,k} - F_{i-1,k}}{2\Delta x} + O(\overline{\Delta x}^2),$$

$$\frac{\partial F}{\partial t} = \frac{F_{i,k+1} - F_{i,k-1}}{2\Delta t} + O(\overline{\Delta t}^2),$$

$$\frac{\partial^2 F}{\partial x^2} = \frac{F_{i+1,k} - 2F_{i,k} + F_{i-1,k}}{\overline{\Delta x}^2} + O(\overline{\Delta x}^2),$$

$$\frac{\partial^2 F}{\partial t^2} = \frac{F_{i,k+1} - 2F_{i,k} + F_{i,k-1}}{\overline{\Delta t}^2} + O(\overline{\Delta t}^2),$$

$$\frac{\partial^2 F}{\partial x \partial t} = \frac{1}{4\Delta x \Delta t}\{F_{i+1,k+1} - F_{i+1,k-1} - F_{i-1,k+1} + F_{i-1,k-1}\} + O(\overline{\Delta x}\,\overline{\Delta t}),$$

and so forth for higher-order derivatives.

At any calculated time level, the value of a function at the rightmost node cannot be obtained following the general scheme. Instead, it is calculated using the two preceding nodes by mean-value.

The following plots were generated using the explicit finite-difference scheme introduced above for three cases indicated in Tables 1, 2 and 3. Due to stability arguments, the solutions obtained by the used explicit numerical scheme could be calculated only for sufficiently small values of time.

The 2D plots illustrate the values of mechanical displacement, temperature, heat flux and electric potential as functions of time at a fixed location $x = 0.5$. Additionally, 3D plots are provided for the same functions in the domain $0 \leq x \leq 10$ and $0 \leq t \leq 5$.

Relying on the fact noticed by several researchers that the effect of nonlinearity is intimately linked to the nature of the considered thermoelastic solid (C.f. [36]), we have chosen to work with materials belonging to different classes, according to the cases introduced above. Whatever be the chosen material, it is generally accepted that the effect of nonlinearity becomes more noticeable as time grows, so that the nonlinear theory is usually necessary for the description of the continuum for sufficiently large time values.

Case 1: The speed of the coupled thermoelastic wave in the linear theory is approximately equal to one third of that of the heat wave ($v_e \simeq 0.37$). Based on this value, the disturbance are expected to reach the location $x = 0.5$ at which the solution is evaluated approximately at time $t = 1.35$. The delay shown in the figures below concerning the displacement, temperature and heat flux will be somewhat different due to the fact that the speed is not exactly equal to v_e according to (27).

As noted above, this case is characterized by a relatively small specific heat capacity, and by a relatively large thermal relaxation time as compared to the other two cases.

Figures 4, 5, 6 and 7 illustrate the behavior of the solution functions in the time interval $0 \leq t \leq 5$.

The main features of the solution observed at an arbitrary location inside the medium as illustrated in Figs. 4, 5, 6 and 7 are:

1. Existence of time delays taken for the disturbances to reach the location at which the solution is evaluated. The delay shown in Fig. 7 is shorter than the one exhibited in the three other unknowns, thus confirming the existence of two speeds of wave propagation.
2. The Figs. 4, 5 and 6 for the displacement, temperature and heat flux show the slower, coupled thermoelastic wave propagating with speed v_E, with oscillations about the zero that are damped in time. It is most probable that the effects of the fast wave here are much smaller and thus not noticeable.
3. In Figs. 5 and 6, the patterns for the temperature and heat flux are similar, the functions tend asymptotically to zero with damped oscillations.
4. In Fig. 7, the electric potential seems to follow exactly the boundary temperature, but at a much smaller amplitude. No damped oscillations are noticed. This electric disturbance reaches the location $x = 0.5$ earlier than the other three, meaning that it is carried by the fast heat wave traveling with speed v_H. This fact provides means for restoring the shape of the boundary temperature through measurements of the electric potential. The reason for this particular behaviour of the electric disturbance is the nature of the equation of electrostatics as stated earlier, in addition to the special values of the material parameters used in the computations.

The 3D-plot in Fig. 8 shows the wave front and thus confirms the wave nature of the solution.
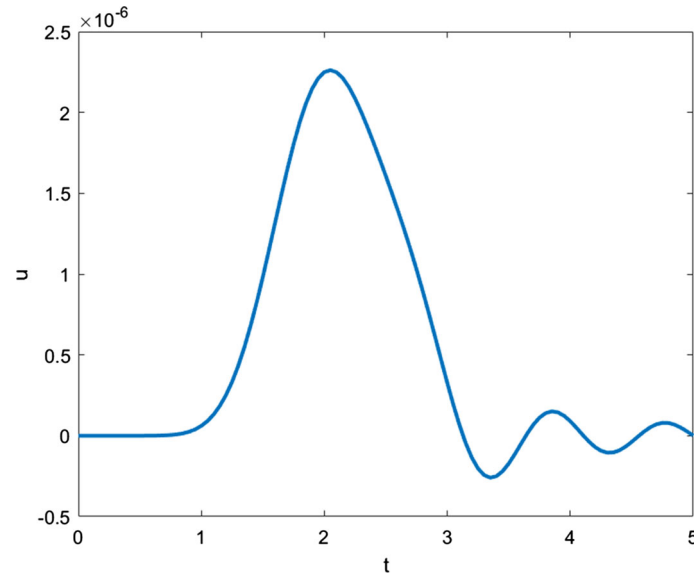
Fig. 4 Distribution of displacement at location $x = 0.5$ as function of time for Case I
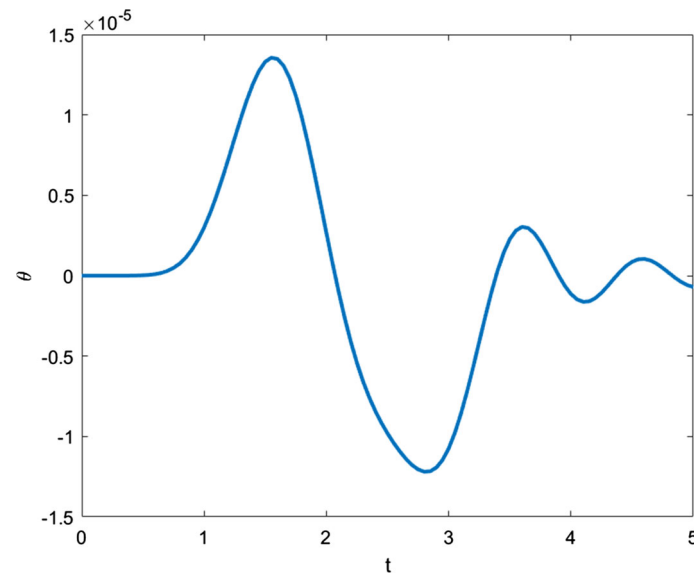

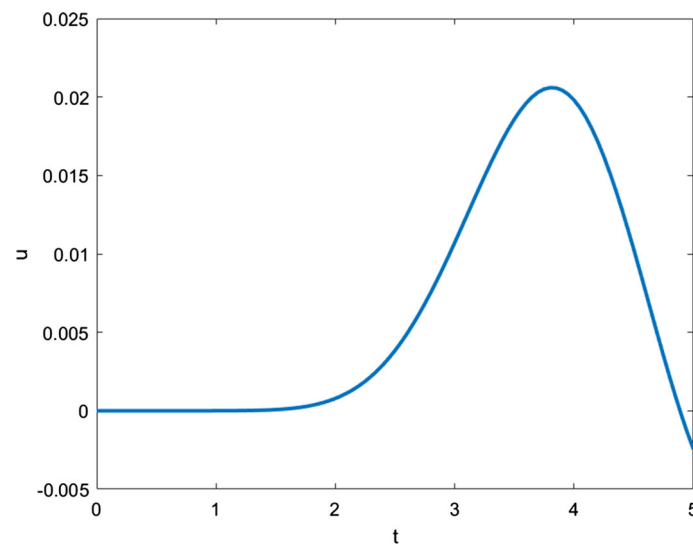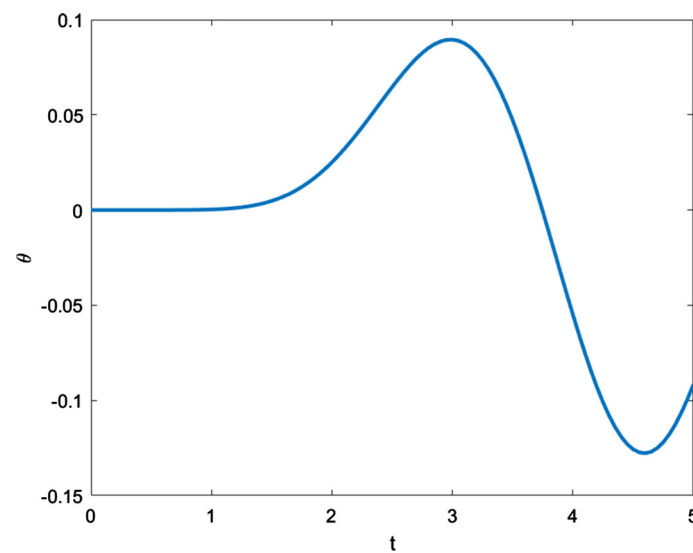**Fig. 5** Distribution of temperature at location $x = 0.5$ as function of time for Case I

Case 2: The dimensionless speed of the coupled thermoelastic wave is approximately equal to ($v_e \simeq 0.16$). Thus the wave is slower than for case I, and six time slower than the heat wave. As time is limited to values $t \leq 5$ for stability reasons of the numerical scheme, Figs. 9, 10 and 11 does not allow to follow the full development of the wave. The behaviour of the electric potential in Fig. 12 looks similar to the corresponding figure for Case I. This electric disturbance has already completely passed by the location $x = 0.5$ while the thermoelastic disturbances are just beginning to appear.

The 3D-plots in Figs. 13, 14, 15 and 16 show distributions of the unknown functions in space and time. In particular, the plot for the electric potential illustrates the oblique wave front in the (x, t)-plane to confirm the existence of the fast wave. This figure confirms that the electric potential follows the shape of the boundary temperature.

Case 3: The dimensionless speed of the linear coupled thermoelastic wave in this case is $v_e \simeq 0.43$. According to Table 1, this case has the largest value of specific heat capacity C_e and the smallest value of the
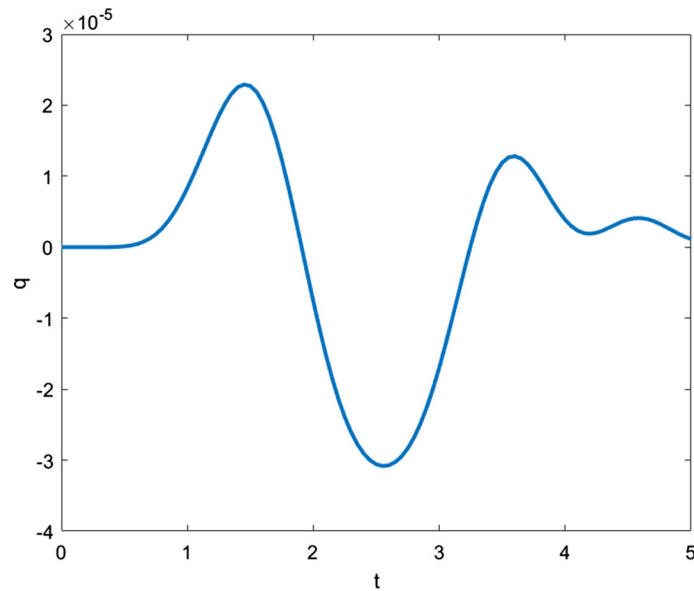
Fig. 6 Distribution of heat flux at location $x = 0.5$ as function of time for Case I
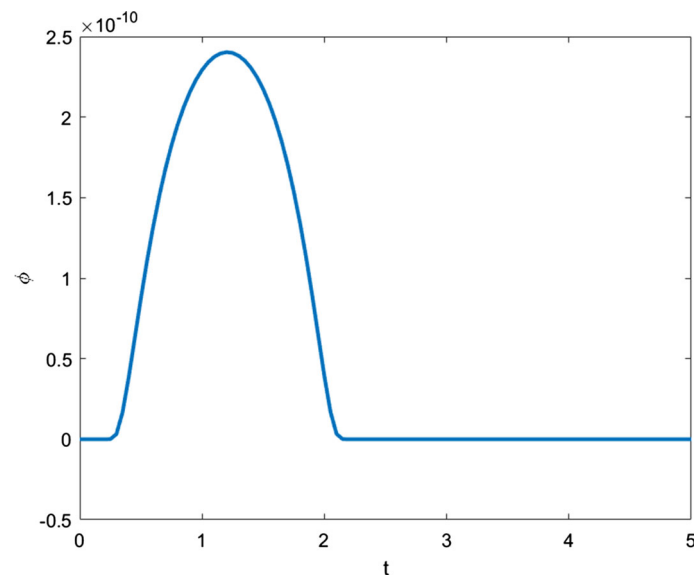
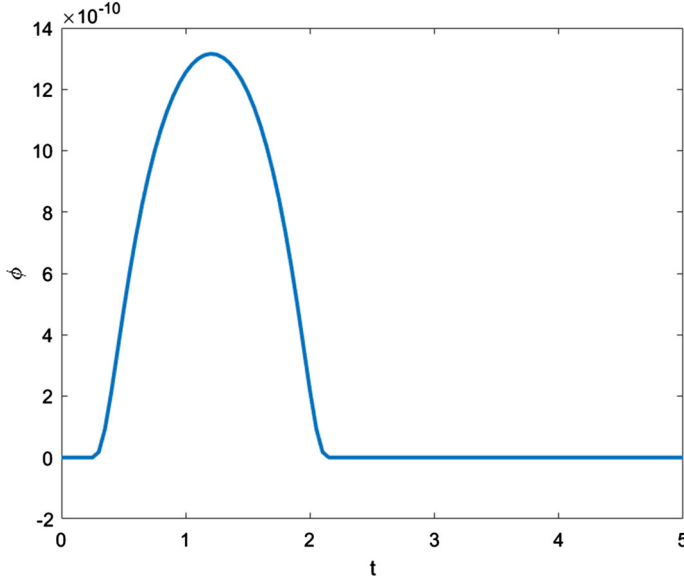**Fig. 7** Distributions of electric potential at location $x = 0.5$ as function of time for Case I

characteristic thermal relaxation time τ_0. Figures 17, 18, 19 and 20 illustrate the behavior patterns of all four solution functions. Here again, one notices the asymptotic behavior of damped oscillations as time grows.

Comparison between the cases:
Figures 21, 22, 23 and 24 illustrate this comparison. The patterns of the four solution functions are similar in all three cases, the only differences concern the orders of magnitude. It is noted that the responses of the medium are more pronounced in Case II than for the other two cases. This fact allows to design working materials in such a way so as to optimize the different responses of the medium to boundary heating.

We have chosen to work in a half-space so as to avoid any reflected waves. Although the propagating boundary regime is one of heating, the obtained temperature distributions in the half-space in all three considered cases showed oscillations that produced negative temperatures during some time interval, before ultimately tending to zero for large times. To comment about this fact, let us recall what was said in Sect. 2 that the used model is thermodynamically consistent. The purely thermal case treated above showed that temperatures
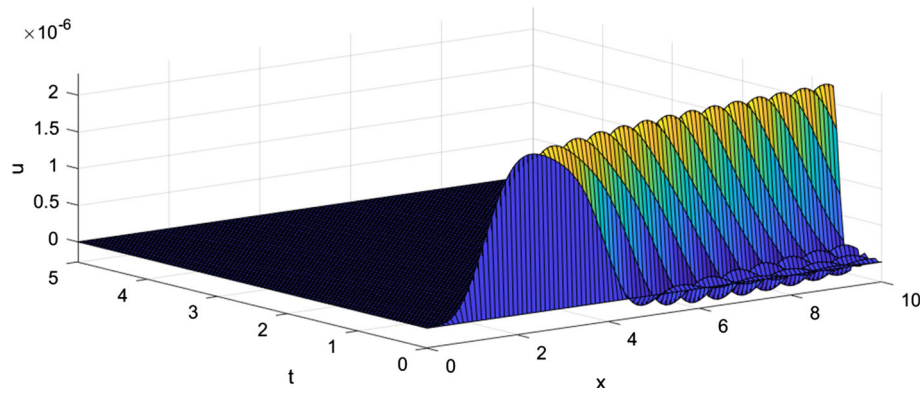
Fig. 8 Three-dimensional displacement distribution for Case I

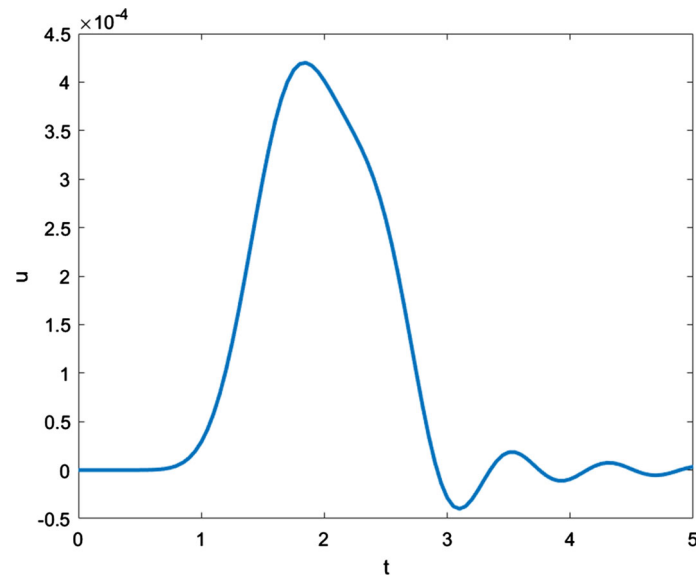**Fig. 9** Distribution of displacement at location $x = 0.5$ as function of time for Case II

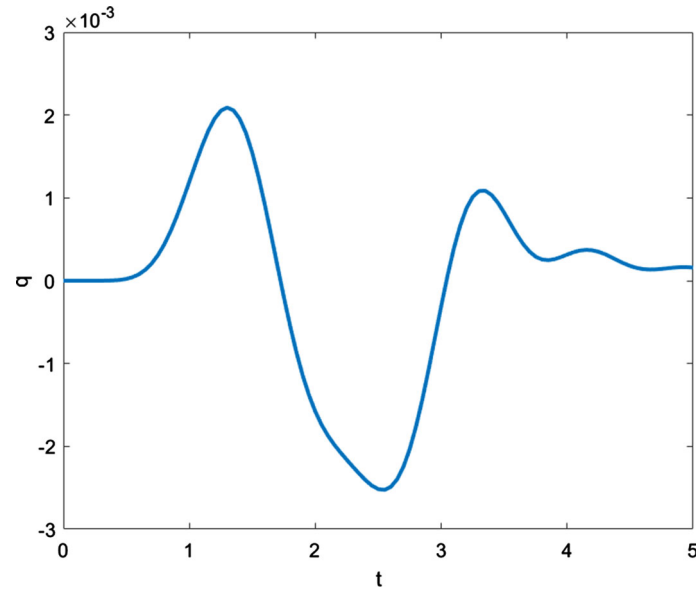**Fig. 10** Distribution of temperature at location $x = 0.5$ as function of time for Case II
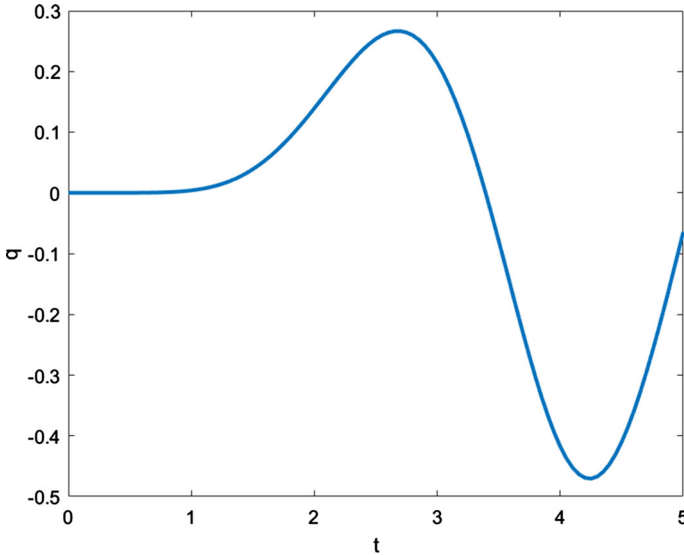
Fig. 11 Distribution of heat flux at location $x = 0.5$ as function of time for Case II

Fig. 12 Distribution of electric potential at location $x = 0.5$ as function of time for Case II
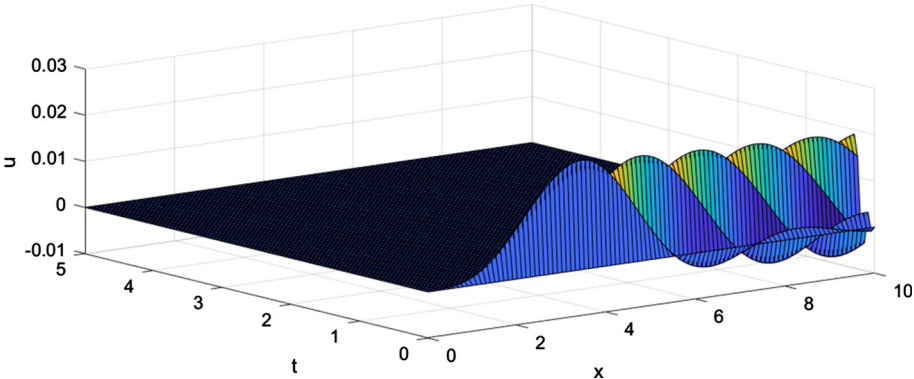
Fig. 13 Three-dimensional distribution of displacement for Case II
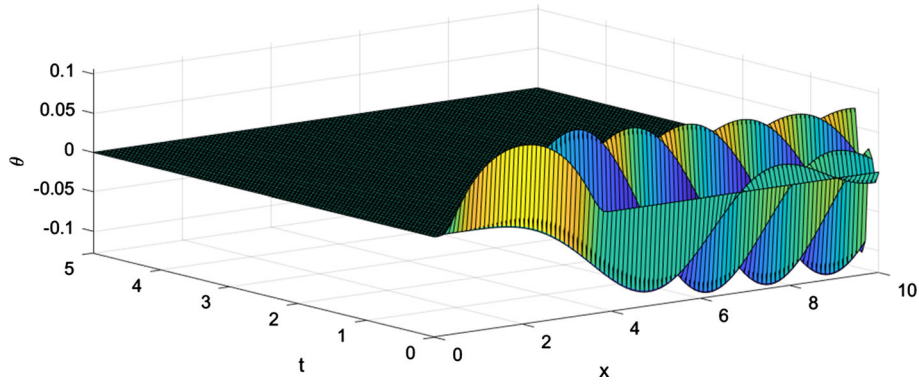
Fig. 14 Three-dimensional distribution of temperature for Case II
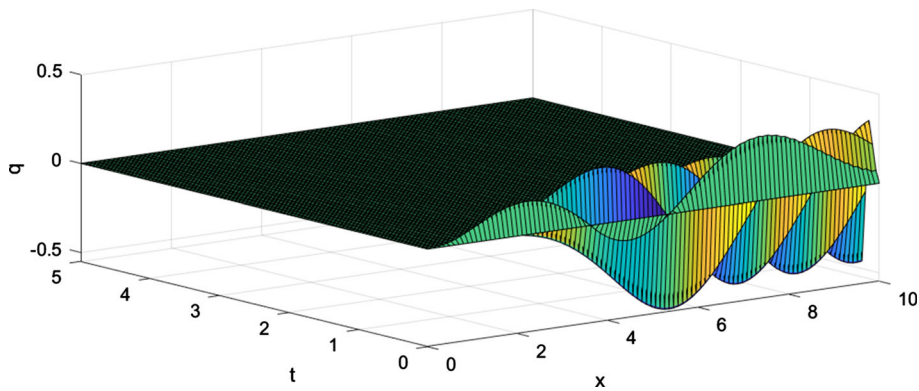
Fig. 15 Three-dimensional distribution of heat flux for Case II
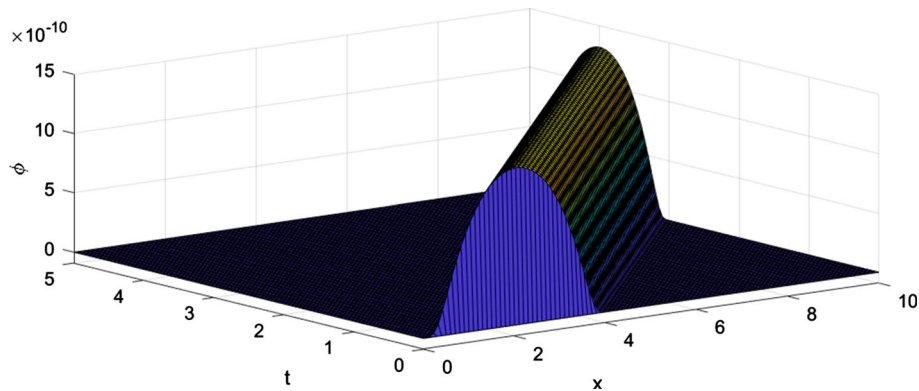
Fig. 16 Three-dimensional distribution of electric potential for Case II

under boundary heating remained non-negative all the time. Along the same line, it was shown in [60] that the arising negative temperatures in a rigid thermal conductor under dual-phase-lag could be made to disappear by properly choosing the values of the relaxation times. For thermoelasticity problems, within the linear Green and Lindsay theory, negative temperature were reported in half-space or square plates subjected to thermal shock or traction by Tehrani and Eslami [61] (Figs.11 and 14 in the cited reference). On the other hand, Abbas and Youssef [62], then Kiani and Eslami [63] investigated nonlinear thermoelasticity of a half-space or layer subjected to thermal shock under Lord-Shulman theory and obtained non-negative temperatures. Generally, it is known that temperature decrease can be attributed to the various thermo-mechanical interactions (linear or nonlinear) and the accompanying energy transfer. Referring to the present results, any conflict with the second law of Thermodynamics is ruled out.

Fig. 17 Distribution of displacement at location $x = 0.5$ as function of time for Case III
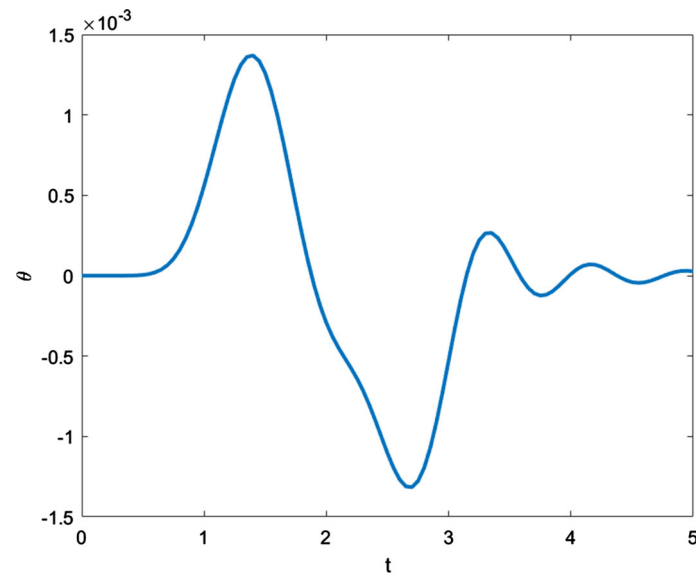
Fig. 18 Distribution of temperature at location $x = 0.5$ as function of time for Case III

Three classes of electro-thermoelastic materials occupying a half-space were considered for the behavior under heating boundary regime. Irrespective of the amplitudes, the solutions for the displacement, temperature and heat flux have all shown evidence of the slow, coupled thermoelastic wave progressing in depth, not of the fast heat wave. At any location, these three functions were characterized by oscillations that damped with time. The fast heat wave could be put in evidence only through the electric potential.

7 Conclusions

The present work aims at assessing the effect of several nonlinear couplings between the mechanical, thermal and electric fields in materials with complex structure used in the various applications. It is known that nonlinearities may affect the efficiency of certain thermoelastic parts in technological structures subjected to mechanical, thermal and electrical loads in working situations. Based on an existing model of nonlinear thermo-

Fig. 19 Distribution of heat flux at location $x = 0.5$ as function of time for Case III
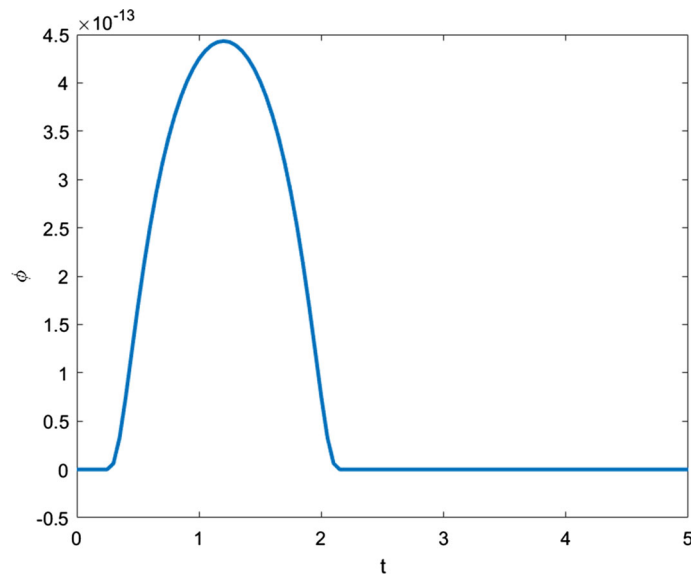
Fig. 20 Distribution of electric potential at location $x = 0.5$ as function of time for Case III

electroelasticity in extended thermodynamics, we have investigated a one-dimensional system of nonlinear partial differential equations, in order to assess the effect of the different coupling constants on the behavior of the medium under thermal load. Such one-dimensional models are easier to analyze mathematically, in particular in relation to existence and uniqueness of solutions, and at the same time can reveal new aspects of the solution as efficient approximations to higher dimensions. The development of nonlinear models of thermoelasticity in extended thermodynamics may help determining the values of some material constants experimentally using heat wave propagation.

Explicit formulae are given for the specific heat capacity, and for the speeds of the coupled thermoelastic wave and the heat wave, showing their dependence on strain, temperature, heat flux and electric field in the nonlinear theory. These formulae have not been mentioned previously. They may be used to determine experimentally some material constants of the medium.

The presented two- and three-dimensional plots for the different unknown functions and for different sets of values of the material coefficients show the wave propagation nature of the solution. They allow to assess
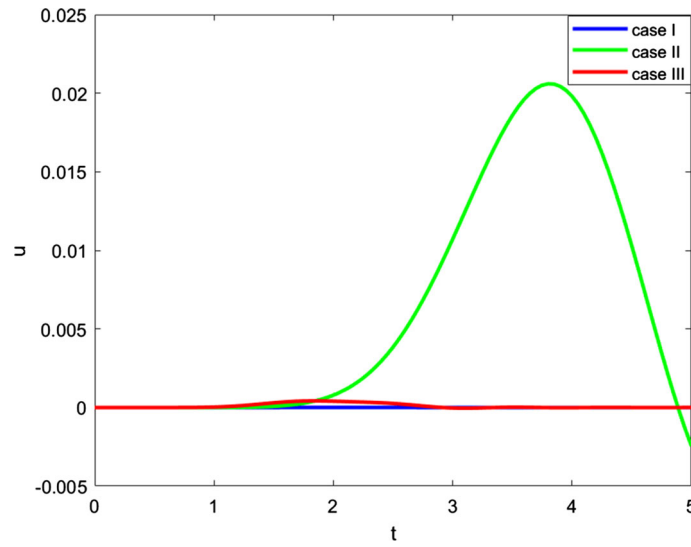
Fig. 21 Comparison of distributions for displacement at location $x = 0.5$ as functions of time for three cases
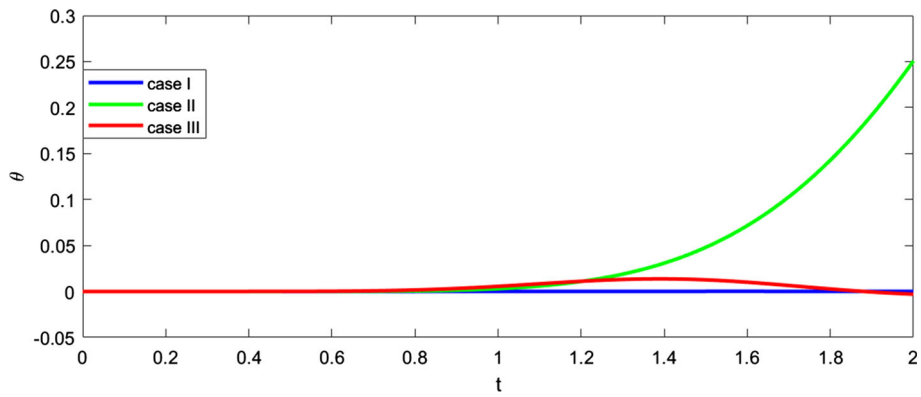
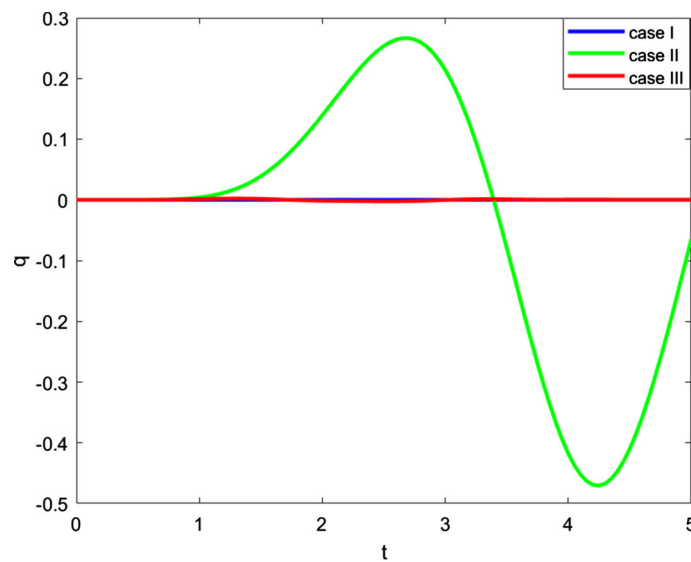**Fig. 22** Comparison of distributions for temperature at location $x = 0.5$ as functions of time for three cases

Fig. 23 Comparison of distributions for heat flux at location $x = 0.5$ as functions of time for three cases
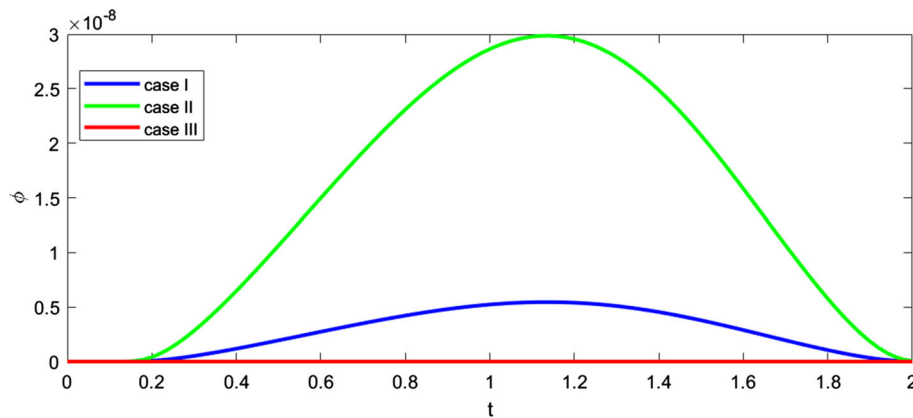
Fig. 24 Comparison of distributions for electric potential at location $x = 0.5$ as functions of time for three cases

the effect of the various coupling constants on the behavior of the mechanical, thermal and electric properties of the medium. It is noted that the responses of the medium are more pronounced in Case II than for the other two cases. This case is characterized by larger values of the piezoelectric coefficient, stronger electrostriction, stronger dependence of the specific heat capacity and thermoelastic coefficient on electric field, and by weaker dependence of the specific entropy on the electric field, weaker dependence of the permanent polarization on strain and on the product of strain and temperature.

It was noticed that the displacement, temperature and heat flux have all shown evidence of the slow, coupled thermoelastic wave. At any particular location in the half-space, these functions had an oscillatory that damped with time. Only the electric potential has shown evidence of the fast heat wave and followed the same behavior of the boundary heat regime irrespective of the amplitude.

The present approach through one-dimensional equations has been efficiently used to reveal important information about the nonlinear couplings in thermoelastic media within extended thermodynamics. The obtained results may be of interest for the design of new electro-thermoelastic materials with specific characteristics. They confirm the fact that the effects of nonlinearity are intimately linked to the nature of the considered thermoelastic medium.

Data availability All data generated or analyzed during this study are included in this article

Declarations

Conflict of interest The authors declare that they have no conflict of interest.

References

1. Eringen, A.C., Maugin, G.A.: Electrodynamics of Continua: Foundations and Solid Media. Springer, New York (1990). https://doi.org/10.1007/978-1-4612-3226-1
2. Yang, J. S.: An introduction to the theory of piezoelectricity. In: Advances in Mechanics and Mathematics, vol. 9. Springer (2005). https://doi.org/10.1007/978-3-030-03137-4

3. Dorfmann, A., Ogden, R.W.: Nonlinear electroelasticity. Acta Mech. **174**, 167–183 (2005). https://doi.org/10.1007/s00707-004-0202-2

4. Dorfmann, A., Ogden, R.W.: Nonlinear electroelastic deformations. J. Elast. **82**, 99–127 (2006). https://doi.org/10.1007/s10659-005-9028-y

5. Muliana, A.: Time dependent behavior of ferroelectric materials undergoing changes in their material properties with electric field and temperature. Int. J. Solids Struct. **48**, 2718–2731 (2011). https://doi.org/10.1016/j.ijsolstr.2011.05.021

6. Dorfmann, L., Ogden, R.W.: Nonlinear Theory of Electroelastic and Magnetoelastic Interactions. Springer, New York (2014). https://doi.org/10.1007/978-1-4614-9596-3

7. Lin, C.-H., Muliana, A.: Nonlinear electro-mechanical responses of functionally graded piezoelectric beams. Compos. Part B Eng. **72**, 53–64 (2015). https://doi.org/10.1016/j.compositesb.2014.11.030

8. Dorfmann, L., Ogden, R.W.: Nonlinear electroelasticity: material properties, continuum theory and applications. Proc. R. Soc. A Math. Phys. Eng. Sci. **56**, 1–34 (2017). https://doi.org/10.1098/rspa.2017.0311

9. Wu, B., Zhang, C., Zhang, C., Chen, W.: Theory of electroelasticity accounting for biasing fields: retrospect, comparison and perspective. Adv. Mech. **46**, 1 (2016). https://doi.org/10.6052/1000-0992-15-020

10. Coleman, B.D., Fabrizio, M., Owen, D.R.: On the thermodynamics of second sound in dielectric crystals. Arch. Ration. Mech. Anal. **80**, 135–158 (1982). https://doi.org/10.1007/BF00250739

11. Coleman, B.D., Fabrizio, M., Owen, D.R.: Thermodynamics and the constitutive relations for second sound in crystals. In: Serrin, J. (ed.) New Perspectives in Thermodynamics. Springer, Berlin (1986)

12. Coleman, B.D., Newman, D.C.: Implications of a nonlinearity in the theory of second sound in solids. Phys. Rev. B **37**(4), 1492–1498 (1988). https://doi.org/10.1103/PhysRevB.37.1492

13. Chandrasekharaiah, D.S.: A generalized linear thermoelasticity theory for piezoelectric media. Acta Mech. **71**, 39–49 (1988). https://doi.org/10.1007/BF01173936

14. He, T., Cao, L., Li, S.: Dynamic response of a piezoelectric rod with thermal relaxation. J. Sound Vib. **306**(3–5), 897–907 (2007). https://doi.org/10.1016/j.jsv.2007.06.018

15. Babaei, M.H., Chen, Z.T.: Dynamic response of a thermopiezoelectric rod due to a moving heat source. Smart Mater. Struct. **18**(2), 025003 (2008). https://doi.org/10.1088/0964-1726/18/2/025003

16. Montanaro, A.: On the constitutive relations for second sound in thermo-electroelasticity. Arch. Mech. **63**(3), 225–254 (2011). https://doi.org/10.48550/arXiv.0912.1252

17. Ghaleb, A.F.: Coupled thermoelectroelasticity in extended thermodynamics. In: Hetnarski, R.B. (ed.) Encyclopedia of Thermal Stresses (C), pp. 767–774. Springer, Berlin (2014). https://doi.org/10.1007/978-94-007-2739-7

18. Kuang, Z.B.: Theory of Electroelasticity. Springer, Berlin (2014)

19. Montanaro, A.: A Green–Naghdi approach for thermo-electroelasticity. J. Phys. Conf. Ser. **633**, 012129 (2015). https://doi.org/10.1088/1742-6596/633/1/012129

20. Gorgi, C., Montanaro, A.: Constitutive equations and wave propagation in Green–Naghdi type II and III thermoelectroelasticity. J. Therm. Stress. **39**(9), 1051–1073 (2016). https://doi.org/10.1080/01495739.2016.1192848

21. Mehnert, M., Hossain, M., Steinmann, P.: On nonlinear thermo-electro-elasticity. Proc. R. Soc. A **472**, 20160170 (2016). https://doi.org/10.1098/rspa.2016.0170

22. Mehnert, M., Pelteret, J.P., Steinmann, P.: Numerical modelling of nonlinear thermo-electro-elasticity. Math. Mech. Solids **22**(11), 2196–2213 (2017). https://doi.org/10.1177/1081286517729867

23. Kuang, Z.B.: Energy principles for temperature varied with time. Int. J. Therm. Sci. **120**, 80–85 (2017). https://doi.org/10.1016/j.ijthermalsci.2017.03.030

24. Montanaro, A.: On thermo-electro-mechanical simple materials with fading memory. Meccanica **52**, 3023–3031 (2017). https://doi.org/10.1007/s11012-017-0640-2

25. Ghaleb, A.F., Abou-Dina, M.S., Rawy, E.K., El-Dhaba, A.R.: A model of nonlinear thermo-electroelasticity in extended thermodynamics. Int. J. Eng. Sci. **119**, 29–39 (2017). https://doi.org/10.1016/j.ijengsci.2017.06.010

26. Rawy, E.K.: A one-dimensional nonlinear problem of thermoelasticity in extended thermodynamics. Results Phys. **9**, 787–792 (2018). https://doi.org/10.1016/j.rinp.2018.03.040

27. Abou-Dina, M.S., Ghaleb, A.F.: A one-dimensional model of thermo-electroelasticity in extended thermodynamics. SQU J. Sci. **23**(1), 1–7 (2018)

28. Chirilă, A., Marin, M., Montanaro, A.: On adaptive thermo-electro-elasticity within a Green–Naghdi type II or III theory. Contin. Mech. Thermodyn. **3**, 1453–1475 (2019). https://doi.org/10.1007/s00161-019-00766-2

29. Vatulyan, A., Nesterov, S., Nedin, R.: Some features of solving an inverse problem on identification of material properties of functionally graded pyroelectrics. Int. J. Heat Mass Transf. **128**, 1157–1167 (2019). https://doi.org/10.1016/j.ijheatmasstransfer.2018.09.084

30. Mahmoud, W., Moatimid, G.M., Ghaleb, A.F., Abou-Dina, M.S.: Nonlinear heat wave propagation in a rigid thermal conductor. Acta Mech. **231**, 1867–1886 (2020). https://doi.org/10.1007/s00707-020-02628-4

31. Zeverdejani, P.K., Kiani, Y.: Nonlinear generalized thermoelasticity of FGM finite domain based on Lord-Shulman theory. Waves Random Complex Media **32**(2), 575–596 (2020). https://doi.org/10.1080/17455030.2020.1788746

32. Mirparizi, M., Fotuhi, A.R., Shariyat, M.: Nonlinear coupled thermoelastic analysis of thermal wave propagation in a functionally graded finite solid undergoing finite strain. J. Therm. Anal. Calorim. **139**, 2309–2320 (2020). https://doi.org/10.1007/s10973-019-08652-4

33. Jani, S.M.H., Kiani, Y.: Generalized thermo-electro-elasticity of a piezoelectric disk using Lord-Shulman theory. J. Therm. Stress. **43**(4), 473–488 (2020). https://doi.org/10.1080/01495739.2020.1718044

34. Shakeriaski, F., Ghodrat, M.: The nonlinear response of Cattaneo-type thermal loading of a laser pulse on a medium using the generalized thermoelastic model. Theor. Appl. Mech. Lett. **10**, 286–297 (2020). https://doi.org/10.1016/j.taml.2020.01.030

35. Shakeriaski, F., Salehi, F., Ghodrat, M.: Modified G-L thermoelasticity theory for nonlinear longitudinal wave in a porous thermoelastic medium. Phys. Scr. **96**, 18 (2021). https://doi.org/10.1088/1402-4896/ac1aff

36. Luo, J., Wu, S., Hou, S., Moradi, Z., Habibi, M., Khadimallah, M.A.: Thermally nonlinear thermoelasticity of a one-dimensional finite domain based on the finite strain concept. Eur. J. Mech. A/Solids **96**, 13 (2022). https://doi.org/10.1016/j.euromechsol.2022.104726

37. Karmakar, S., Sahu, S.A., Goyal, S.: Wave scattering of plane wave at the loosely bonded interface of two dissimilar rotating triclinic magneto-thermoelastic media under nonlinear thermoelasticity and DPL model. J. Stress. Therm. (2022). https://doi.org/10.1080/01495739.2022.2102555

38. Tarabek, M.A.: On the existence of smooth solutions in one-dimensional nonlinear thermoelasticity with second sound. Q. Appl. Math. **50**(4), 727–742 (1992). https://doi.org/10.1090/qam/1193663

39. Messaoudi, S.A., Said-Houari, B.: Blowup of solutions with positive energy in nonlinear thermoelasticity with second sound. J. Appl. Math. **3**, 201–211 (2004). https://doi.org/10.1155/S1110757X04311022

40. Senousy, M.S., Li, F.X., Mumford, D., Gadala, M., Rajapakse, R.K.N.D.: Thermo-electro-mechanical performance of piezoelectric stack actuators for fuel injector applications. J. Intell. Mater. Syst. Struct. **20**(4), 387–399 (2009). https://doi.org/10.1177/1045389X08095030

41. Yarali, E., Noroozi, R., Yousefi, A., Bodaghi, M., Baghani, M.: Multi-trigger thermo-electro-mechanical soft actuators under large deformations. Polymers **12**(2), 489 (2020). https://doi.org/10.3390/polym12020489

42. Li, X., Lu, S.G., Chen, X.Z., Gu, H., Qian, X.S., Zhang, Q.M.: Pyroelectric and electrocaloric materials. J. Mater. Chem. C **1**, 23–27 (2013). https://doi.org/10.1142/9789811210433_0007

43. Guzmán-Verri, G.G., Littlewood, P.B.: Why is the electrocaloric effect so small in ferroelectrics? APL Mater. **4**(6), 064106 (2016). https://doi.org/10.1063/1.4950788

44. Li, J., Li, J., Wu, H.H., Qin, S., Su, X., Wang, Y., Lou, X., Guo, D., Su, Y., Qiao, L., Bai, Y.: Giant electrocaloric effect and ultrahigh refrigeration efficiency in antiferroelectric ceramics by morphotropic phase boundary design. ACS Appl. Mater. Interfaces **12**(40), 45005–45014 (2020). https://doi.org/10.1021/acsami.0c13734

45. Johari, G.P.: Effects of electric field on the entropy, viscosity, relaxation time, and glass-formation. J. Chem. Phys. **138**, 7 (2013). https://doi.org/10.1063/1.4799268

46. Lee, H.J., Saravanos, D.A.: The effect of temperature dependent material properties on the response of piezoelectric composite materials. J. Intell. Mater. Syst. Struct. **9**, 503–508 (1998). https://doi.org/10.1177/1045389X9800900702

47. Lavrentovich, O.D.: Design of nematic liquid crystals to control microscale dynamics. Liquid Cryst. Rev. **8**(2), 59–129 (2020). https://doi.org/10.1080/21680396.2021.1919576

48. Yadav, S.P., Yadav, K., Lahiri, J., Parmar, A.S.: Ferroelectric liquid crystal nanocomposites: recent development and future perspective. Liquid Cryst. Rev. **6**(2), 143–169 (2021). https://doi.org/10.1080/21680396.2019.1589400

49. Sherief, H.H., Dhaliwal, R.S.: Generalized one-dimensional thermal shock problem for small times. J. Therm. Stress. **4**(3–4), 407–420 (1981). https://doi.org/10.1080/01495738108909976

50. Grysa, K., Kozłowski, Z.: One-dimensional problems of temperature and heat flux determination at the surfaces of a thermoelastic slab: part I: the analytical solutions. Nucl. Eng. Des. **74**(1), 1–14 (1983). https://doi.org/10.1016/0029-5493(83)90135-8

51. Grysa, K., Kozłowski, Z.: One-dimensional problems of temperature and heat flux determination at the surfaces of a thermoelastic slab: part II: numerical analysis. Nucl. Eng. Des. **74**(1), 15–24 (1983). https://doi.org/10.1016/0029-5493(83)90136-X

52. Chandrasekharaiah, D.S.: One-dimensional wave propagation in the linear theory of thermoelasticity without energy dissipation. J. Therm. Stress. **19**(8), 695–710 (1996). https://doi.org/10.1080/01495739608946202

53. Sukesha, R.V., Kumar, N.: Effect of electric field and temperature on dielectric constant and piezoelectric coefficient of piezoelectric materials: a review. Integr. Ferroelectr. **167**(1), 154–175 (2015). https://doi.org/10.1080/10584587.2015.1107383

54. Huang, M., Tunnicliffe, L.B., Zhuang, J., Ren, W., Yan, H., Busfield, J.J.C.: Strain-dependent dielectric behavior of carbon black reinforced natural rubber. Macromolecules **49**(6), 2339–2347 (2016). https://doi.org/10.1021/acs.macromol.5b02332

55. Dehghan, M., Fakhar-Izadi, F.: The spectral collocation method with three different bases for solving a nonlinear partial differential equation arising in modeling of nonlinear waves. Math. Comput. Model. **53**(9), 1865–1877 (2011). https://doi.org/10.1016/j.mcm.2011.01.011

56. Doha, E.H., Bhrawy, A.H., Hafez, R.M., Abdelkawy, M.A.: A Chebyshev–Gauss–Radau scheme for nonlinear hyperbolic system of first order. Appl. Math. Inf. Sci. **8**(2), 535–544 . https://doi.org/10.12785/amis/080211

57. Bhrawy, A.H., Alghamdi, M.A., Alaidarous, E.S.: An efficient numerical approach for solving nonlinear coupled hyperbolic partial differential equations with nonlocal conditions. Abstr. Appl. Anal. (2014). https://doi.org/10.1155/2014/29593614

58. Doha, E.H., Bhrawy, A.H., Abdelkawy, M.A., Hafez, R.M.: Numerical solution of initial-boundary system of nonlinear hyperbolic equations. J. Pure Appl. Math. **46**(5), 647–668 (2015). https://doi.org/10.1007/s13226-015-0152-5

59. Abdel Gawad, H.I., Abou-Dina, M.S., Ghaleb, A.F., Tantawy, M.: Heat traveling waves in rigid thermal conductors with phase lag and stability analysis. Acta Mech. **233**, 2527–2539 (2022). https://doi.org/10.1007/s00707-022-03241-3

60. Ahmed, E.A.A., Abou-Dina, M.S., Ghaleb, A.F.: Two-dimensional heat conduction in a rigid thermal conductor within the dual-phase-lag model by one-sided Fourier transform. Waves Random Complex Media **32**(5), 2485–2498 (2022). https://doi.org/10.1080/17455030.2020.1854492

61. Tehrani, P.H., Eslami, M.R.: Boundary element analysis of Green and Lindsay theory under thermal and mechanical shock in a finite domain. J. Therm. Stress. **23**, 773–792 (2000). https://doi.org/10.1080/01495730050192400

62. Abbas, I.A., Youssef, H.M.: A nonlinear generalized thermoelasticity model of temperature-dependent materials using finite element method. Int. J Thermophys. **33**, 1302–1313 (2012). https://doi.org/10.1007/s10765-012-1272-3

63. Kiani, Y., Eslami, M.R.: Nonlinear generalized thermoelasticity of an isotropic layer based on Lord-Shulman theory. Eur. J. Mech. A/Solids **61**, 245–253 (2017). https://doi.org/10.1016/j.euromechsol.2016.10.004